Received 4 September 2024; revised 1 October 2024; accepted 9 October 2024. Date of publication 14 October 2024; date of current version 24 October 2024.

Digital Object Identifier 10.1109/OJCOMS.2024.3479241

Multi-OLT Multi-Lane PON for 5G Fronthaul and Differential Services Through Access Class Priority-Based 2D Scheduling

FAHMIDA RAWSHAN [1] (Member, IEEE), MONIR HOSSEN [2] (Senior Member, IEEE), AND MD. RAFIQUL ISLAM [1] (Member, IEEE)

[1]Department of Electrical and Electronic Engineering, Khulna University of Engineering and Technology, Khulna 9203, Bangladesh
[2]Department of Electronics and Communication Engineering, Khulna University of Engineering and Technology, Khulna 9203, Bangladesh

CORRESPONDING AUTHOR: M. HOSSEN (e-mail: mhossen@ece.kuet.ac.bd)

The work of Fahmida Rawshan was supported by the University Grants Commission of Bangladesh through the UGC Fellowship for Ph.D. Program.

ABSTRACT Optical and wireless convergence is a quest of time. The rising bandwidth demand focuses on optical technology while increasing mobile bandwidth access requires wireless connectivity. Network convergence is a must to go through the solution. Multi-optical line terminal (multi-OLT) passive optical network (PON) has gained consideration for this solution for its widespread integration aptitudes. This paper proposes a multi-OLT multi-lane PON-based access network that provides service to the fifth-generation (5G) centralized radio access network (C-RAN) fronthaul on top of the existing access services. The design follows 100 Gb/s next-generation Ethernet passive optical network (NG-EPON) standards along with an optical network unit (ONU) structure to provoke dynamic channel bonding. A novel wavelength and bandwidth allocation scheme named access class priority-based 2D scheduling (ACP-2D) for upstream traffic is also designed. Computer simulations are performed to justify the performance of the ACP-2D scheme in a mini-slot-based 5G new radio (5G NR). Four different service providers (SPs) occupy four different OLTs. The services provided by the SPs are the Internet of Things (IoT), fiber-to-the-home (FTTH), wireless sensor network (WSN), and 5G. Simulation results show that 5G fronthaul traffic is successfully transmitted (owing to the full desired throughput of 0.798) within the 3GPP delay requirement of 250 μsec while maintaining other services. For example, the maximum FTTH service jitter is achieved to be 0.26 μsec for a maximum delay of 546.94 μsec at a mini-slot of 250 μsec. Network upstream bandwidth utilization is achieved by about 99.9%, which indicates a very small amount of network overhead. This innovative work signifies that multi-OLT PON can promote acceleration on the journey from C-RAN to open RAN.

INDEX TERMS 5G, C-RAN, DWBA, FTTH, multi-OLT, NG-EPON, optical and wireless convergence, O-RAN, PON.

I. INTRODUCTION

NOWADAYS, tablets and smartphones are used frequently for accesing the broadband Internet rather than a desktop. Emerging applications related to virtual and augmented reality, healthcare, and automotive are speed and bandwidth haunted [1], [2]. The tradeoff between user connectivity and usage patterns demands optical and wireless convergence at the physical network level. The core level convergence can further be promoted by software defined networking and network functions virtualization (NFV) technologies [3]. Network slicing can separate the central control plane from the data plane and manage mobility from fixed to mobile services. It leverages capital expenditures (CAPEX) on separate infrastructure for different access types.

The key requirement of the fifth-generation (5G) radio access technology is to overcome the distributed propensity of the fourth-generation (4G) system by enabling coordinated

multi-point (CoMP) among densified cells, expounding spectrum into millimeter wave, and using massive multiple-input multiple-output (m-MIMO) antenna technology [4], [5]. The air interface selected for 5G is labeled as 5G New Radio (5G NR). To envisage 5G requirements, the baseband unit (BBU) is further divided into two functional blocks called central unit (CU) and digital unit (DU). Moreover, the remote radio unit (RRU) is renamed as a remote unit (RU). CU is moved to the core network and thus creates a new interface termed midhaul between CU and DU. Backhaul is the transport between the CU and the core network. The mobile fronthaul in 5G is between DU and RU with increasing lengths up to 20 km. Among the three transports, fronthaul has the most rigorous requirements.

The fronthaul concept enabled a centralized radio access network (C-RAN) which is reported to save 40-50% of energy using the existing radio access network (RAN) equipment [6]. Common public radio interface (CPRI) is the most used fronthaul protocol by RAN vendors. The 3rd Generation Partnership Project (3GPP) re-defined CPRI functional split options to address 5G NR challenges [7]. They can lessen pressure on fronthaul and enable packet-based transmission with statistical multiplexing [3]. This situation further triggers salutation for optical and wireless convergence. C-RAN can be directed to virtualized RAN (vRAN) by decoupling the software from hardware through NFV. vRAN can further evolve into open RAN (O-RAN) architecture to promote multiple service demands [8]. This evolution path motivated us to design a next-generation fronthaul with multi-OLT passive optical network (PON).

Optical access is mostly deployed through fiber-to-the-home (FTTH) scenarios worldwide. PON is the most demanded FTTH technology for its cost-effective deployment [9]. This existing fiber infrastructure can be used to transport new fronthaul or midhaul supporting massive small cell-based C-RAN [10]. Extensive research has been carried out to transport fronthaul streams through different PON technologies based on time division multiplexing (TDM), wavelength division multiplexing (WDM), and time and wavelength division multiplexing (TWDM). Even multiple optical line terminal (OLT) PON can be an innovative and interesting research topic for 5G fronthauling. PON can be established as a platform for open access if multiple OLTs are added [11]. Open access networks (OANs) are open for different kinds of access services sharing a common fiber infrastructure. Thus, multi-OLT PON can be an evolution partner for C-RAN to start the journey to the next generation O-RAN while maintaining different access services [12].

The multi-OLT PON can better handle the OAN computational complexity, application variety, and device assortment than conventional PON [13], [14], [15]. Multi-OLT PON has been regarded as an outstanding research topic for multi-service providers (SPs) serving end users sharing downstream resources [1]. It could be greatly interesting to investigate the upstream side of these compound OAN when multi-OLT PON is subjected to 5G fronthaul transport along with differential access services. This paper presents a next-generation fronthaul transport with a multi-OLT PON-based access network. The network is designed based on the next-generation Ethernet passive optical network (NG-EPON) having four wavelength lanes each of 25 Gb/s [16]. An optical network unit (ONU) is envisioned to share multiple wavelengths.

A dynamic wavelength and bandwidth allocation (DWBA) algorithm can manage the transmission flexibility of the ONUs in the case of multiple wavelength sharing. The total upstream bandwidth of an ONU can be split over multiple wavelengths in the form of transmission windows. The main challenges in designing a DWBA in NG-EPON can be summarized as – load balancing in multiple wavelengths, transmission overhead managing due to extra guard time usage for an ONU transmitting on multiple wavelengths, reducing frame resequencing delay, and controlling additional delay due to non-fragmentable nature of Ethernet frames. Besides the multi-OLT PON-based fronthaul, we proposed an appropriate operational scheme named access class priority-based 2D scheduling (ACP-2D) to manage the aforementioned challenges.

Network disaggregation approaches are becoming popular which makes it challenging to fill a 100G link for a single ONU [17]. Thereby, a new design for special purpose ONU is presented in the research which is marked as platinum (P) class ONU. The P-class ONU can leverage dynamic channel bonding over four lanes to aggregate a 100G service rate if necessary. Our previous research work proposed silver (S) class and gold (G) class ONUs that coexist in the network for modest operations [1]. The existence of such ONUs from different generations in a network can create optical level mismatch problems and upsurge costs in single OLT architecture (i.e., 1+3 architecture) [8]. Multiple OLTs of different generations connected to ONUs of the same generation can better handle this challenge. Thereby in the proposed network, four SPs reside with four OLTs and are connected to the corresponding access subscriber class. The provided four services through the SPs are selected as 5G, Internet of Things (IoTs), FTTH, and wireless sensor network (WSN). The main contributions of this paper can be concisely described as follows:

- A novel multi-OLT multi-lane PON-based access network is designed to support 5G fronthaul and multi-access.
- Multiple OLTs are proposed with service-based capacity to deliver differential services provided by diverse SPs.
- An ONU grouping into different service classes is suggested to support services through a combination of OLTs.
- An ONU structure is proposed to deliver 5G service which can aggregate peak 100 Gb/s data rate through channel bonding.
- A new DWBA scheme is proposed to handle the upstream operation of the multi-OLT multi-lane

PON-based access system along with 5G fronthaul for C-RAN.
- Dynamic channel bonding is incorporated with the DWBA scheme to extend upstream services.

The rest of this paper is organized as follows. Section II represents an important literature review. The network architecture and ONU design are presented in Section III. The proposed ACP-2D scheme is depicted in Section IV. Section V presents the simulation results in detail. Finally, conclusions are presented in Section VI.

II. LITERATURE REVIEW

Numerous types of the research reported success of the PON system in carrying fronthaul streams of 5G C-RAN satisfying strict latency requirements of 250 μsec. Academia and industry-focused both on IEEE NG-EPON and ITU-T next generation-PON (NG-PON2) for deploying fronthaul. Applicable dynamic bandwidth allocation (DBA) algorithms for the operation of such PON are another topic of concern. Multi-OLT multi-lane PON could be an added in the way to show innovative solutions in upcoming open-access open-vendor RAN systems. This section presents the important research initiations yet and the upcoming possibilities. The 1st subsection presents PON-based fronthaul and the 2nd subsection shows algorithms necessary to operate PON.

A. PON-BASED FRONTHAUL

Tashiro et al. in [18] presented the first experimental study that reports TDM-PON upstream latency diminution satisfying fronthaul requirements. This achievement was demonstrated using a 10G-EPON prototype through mobile-DBA that cooperates through BBU mobile-scheduling information. Uzawa et al. in [19] proposed a practical mobile DBA scheme enabling proper time slot allocation by data-arrival period estimation. The NG-PON2 system-based experimentation presented low-latency mobile fronthaul transmission. 5G fronthaul and secondary services are accommodated in a TDM-PON without additional interface in the studies of [20], [21]. A traffic monitor is used to confine the mobile fronthaul signal and estimate insertion opportunities for secondary services to build a cost-effective fronthaul. These researchers attempt to recover the estimation error.

Nakayama and Hisano in [22] proposed a TWDM-PON to support mobile fronthaul. The upstream fronthaul traffic is supported by the designed wavelength and bandwidth allocation algorithm which enables minimalizing the number of active wavelength channels. The algorithm accommodates TDD-based fronthaul streams satisfying the strict latency requirements. The leading point of the TTI cycle is forecasted at the OLT through a traffic monitor. The algorithm allocates fixed bandwidth in fixed channels considering the worst-case (maximum burst) transmission. Uzawa et al. in [23] presented a TDM-PON to accommodate mobile fronthaul and IoT networks on different network slices. A DBA scheme is designed to virtually isolate these two sub-networks with different requirements. Experimental results show that the scheme continued low-latency fronthaul transmission while serving guaranteed bandwidth to IoT and performing an auto-discovery process for newly connected ONUs.

NG-EPON aggregates multiple wavelength channels through channel bonding features to achieve peak data rate in ONU. Self-adjusting DBA algorithm is designed to deliver 5G fronthaul services without interrupting data services in NG-PON [24]. Multiple wavelengths are bonded to serve 5G fronthaul services in [25]. All the wavelengths are initially assigned to ONUs using a long-standing traffic demand prediction for wavelength assignment for ONU channel bonding. The study in [26] considered a TWDM-PON for fixed and mobile platform convergence. An integrated cooperative and status-report DWBA-type algorithm based on wavelength and bandwidth preemption (WBP) is used for this purpose. In mini-slot-based 5G NR, resource allocation conflict happens during the integration process. A conflicted time-sensitive fronthaul traffic is preempted by the wavelength and bandwidth allocated to the other types of traffic during confliction.

B. DWBA ALGORITHMS OF NG-EPON

A DWBA scheme can truly realize the transmission litheness of ONU in the case of multi-wavelength lane transmission as the total upstream bandwidth of the ONU is split over multiple lanes in the form of transmission slots. DWBA designing for NG-EPON can be challenging due to load balancing, transmission overhead managing, resequencing delay reducing, and non-fragmentable Ethernet frame format. Several schemes deal with these issues from different perspectives.

Wang et al. in [27] proposed the water-filling DWBA (WF-DWBA) algorithm for NG-EPON to leverage for balancing load in all four wavelengths. The algorithm allocates bandwidth to an ONU on several wavelengths based on its demand starting from the least utilized channel. Hussain et al. in [28] proposed the first-fit DWBA (FF-DWBA) algorithm to improve bandwidth utilization while reducing the amount of out-of-order frame reception. It tries to allocate ONU grants mostly on a single wavelength. This feature makes FF-DWBA perform well in scenarios when the low load is offered per ONU otherwise WF-DWBA is well performing. Hussain et al. in [29] designed the flexible wavelength and dynamic bandwidth allocation (FW-DBA) algorithm to adapt ONU bandwidth on multiple wavelengths according to its offered load. A DWBA named single channel as possible (SCAP) is designed by Wang et al. in [30] to mitigate the frame-reordering phenomenon. It reports better bandwidth utilization over the WF-DWBA algorithm by allocating a possibly higher number of ONUs over a single wavelength. SCAP rearranges ONU bandwidth requests in descending order and allocates the biggest one in the least crowded wavelength. If the full request is not accommodated then it divides allocation over several wavelengths which still

results in frames out of order reception at OLT. DWBA-FRA also deals with frame-rearrangement problem in [33]. It lowers the number of ONUs facing out-of-order frames than the SCAP scheme. DWBA-FRA arranges ONUs in ascending order of demand and tries to ensure impartial resource distribution among them over four wavelengths promoting load balance. Besides promoting load balance and reducing overhead by excess guard time, peak transmission rate should be achieved to the ONUs in NG-EPON. To keep this in mind, an algorithm is designed based on ONU-load and round trip times (RTTs) by Hui et al. in [34]. Here, the ONUs are grouped according to the load. Low load group transmits in lesser wavelengths while higher load groups transmit in more than one wavelength. Each group shorts the ONUs in ascending order of RTT to reduce idle time. DWBA algorithm based on the ONU's request in sequential order (DWBA-RSO) in the pool is proposed in [35] which decreases the frame-reordering.

In conclusion of this section, it could be said that initial efforts and achievements paved the way to broadly open our sense to seriously think about PON-based fronthaul. Still, the architectures and algorithms have some limitations that are summarized in Table 1. As the PON structure is already deployed to serve data services, it is time to cope with RAN fronthauling on top of existing services with little extension and coordination. Multi-OLT PON has an excellent opportunity in the upcoming O-RAN as it permits multi-service environments. To the best of our knowledge, we are the first to work with multi-OLT PON-based fronthaul for C-RAN. We have designed a novel upstream DWBA scheme ACP-2D in this research to cope with this new environment which considers channel bonding constraints properly. It is good enough at load balancing by defining the same frame limit over multiple wavelengths. It limits transmission overhead due to extra guard time usage for an ONU transmitting on multiple wavelengths. It reduces frame resequencing delay and controls additional delay due to non-fragmentable Ethernet frames.

III. PROPOSED NETWORK ARCHITECTURE

Although IEEE NG-EPON is a single OLT structure, multi-OLT PON-based OAN can be designed following NG-EPON standard [16]. The proposed architecture can cater to pay-as-you-grow, local loop unbundling, service restoration, energy saving, and coexistence of cross-generation optics cost-effectively. The existence of ONUs from different generations (25G, 50G, and/or 100G) in a network can create optical level mismatch and increase cost in single OLT architecture (i.e., 1+3 architecture) [8]. This paper proposes multiple OLTs of different generations in a PON network to handle corresponding grouped ONUs to solve this mismatch issue. Each OLT in the PON can be occupied by a different SP featuring local loop unbundling [36]. The number of SPs can easily be extended as the OLT needs only a single fiber from the splitter location which gives the provision of pay as you grow.

Fig. 1 shows the proposed network architecture with multiple OLTs in the CO location and different ONUs on the subscriber side. CU stands near the core network and is connected to the AP server through a layer 2 switch (L2S). L2S switches packets without interfering with the communication between hosts and destinations by looking at their physical addresses. The F1 interface is used between CU and DU while the Fx is used between DU and RU. As the network has M OLTs at the CO, M number of SPs can be accommodated here. For example, FTTH, IoT, WSN, and 5G wireless SPs occupy the OLT_1, OLT_2, OLT_3, ... OLT_{M-1} and OLT_M, respectively. 5G SP shows two variant connections for two different interfaces shown through OLT_{M-1} and OLT_M. The OLTs can use a modified multi-point control protocol (MPCP) and shared DBA poling table for multi-OLT PON to allocate wavelength and bandwidth to the subscribers connected to ONUs [13].

The proposed class-based differential access shown in Fig. 1 is a standing platform for a mixed generation of ONUs. The ONUs are grouped according to their service class subscriptions. The 1st generation ONUs are virtually grouped under the S-class. In the figure, ONU-S represents this class and provides an access point (AP) from IoT SP in a single wavelength pair (λ_1, λ_1'). The 2nd generation gold-class (G2) ONUs, i.e., ONU-G2 can access WSN and FTTH SPs in wavelength pair (λ_2, λ_2'). The 3rd generation gold-class (G3) ONUs can access three SPs using these two wavelength pairs independently. These device structures have been already designed using fixed optics [1]. This paper proposes the structure of the 4th generation P-class ONUs (which is further divided into ONU-P1 and ONU-Px according to the 5G interface (F1/Fx). Fig. 2 summarizes the capacity range and access categories for 25G ONU-S and ONU-G2, 50G ONU-G3, and 100G ONU-P. Generation upgrades in ONUs can easily be achieved through line card swapping. ONU-S has strict access from a single SP in the upstream wavelength λ_1'. ONU-G2 enjoys sharing access from two SPs at a time in the upstream wavelength λ_2'. ONU-G3 has limited access to three SPs combining λ_1' and λ_2'. However, wavelengths λ_3' and λ_4' are reserved for 5G subscribers belonging to ONU-P. These ONUs can fully cover the wavelength range through channel bonding if necessary.

This paper proposes the structure of the P-class ONU as shown in Fig. 3. Media access control (MAC) block resided beside four fixed λ transceiver arrays. Turning on/off the four sets of wavelengths on a single line card is a handy solution to achieve colorless operation and low cost simultaneously [37]. There are four wavelengths of 25 Gb/s and each wavelength is allocated for the upstream and downstream transmissions, ONU-P can be empowered by dynamic channel bonding to easily achieve a peak upstream rate of 100 Gb/s. The presence of internal MUX makes deployment easier and decreases the loss due to the elimination of two extra connectors. A diplexer is a passive device used here to separate two

TABLE 1. Summary of important recent studies.

Ref.	Year	Contribution	Limitation
[1]	2023	A multi-OLT PON-based OAN is studied with downstream sides.	Need to study upstream and policy for accommodating 5G fronthaul.
[18]	2014	TDM-PON latency met fronthaul requirements for the first time.	The mobile scheduling should be administered about 4 msec before uplink transmission from UE. As the value of this parameter decreases in mini-slot-based 5G NR, it is challenging to utilize.
[19]	2017	A practical mobile DBA scheme with proper time slot allocation is proposed.	An additional interface is needed to connect CU to the OLT. Not always a feasible solution where wireless and wired network operators are different bodies.
[20], [21]	2017, 2018	5G fronthaul and secondary services are accommodated in a TDM-PON.	It takes almost 14 msec to start recovery after estimation error detection. The estimation error period causes delayed fronthaul bursts.
[22]	2019	The upstream fronthaul traffic is supported by wavelength and bandwidth allocation that minimizes active wavelength usage.	A Fixed time slot assignment results in low network utilization for low-loaded ONUs.
[24]	2021	Self-adjusting DBA algorithm delivers 5G fronthaul services along with data services in NG-PON.	The channel bonding constraints are not well considered.
[25]	2022	Channel bonding is presented to serve 5G fronthaul services.	Quality of service degrades if actual traffic deviates from the initial predicted value.
[26]	2022	Mini-slot-based 5G NR is demonstrated.	Preemption causes interruption of secondary services.
[31]	2023	Cost and energy consumption reduction aspects are considered to model a 5G/6G optical fronthaul.	Fronthaul performance parameters are not considered.
[32]	2024	The steps engaged in industries to empower PON-based fronthaul are discussed.	The standardization and technical aspects of converging mobile and fixed access systems are overviewed only.
[27]	2017	WF-DWBA is proposed for NG-EPON multi-lane load balancing.	Bandwidth utilization lowers due to excessive guard time usage.
[28]	2017	Improves NG-EPON bandwidth utilization.	FF-DWBA algorithm is incompetent in terms of litheness of load fluctuation and ONU number.
[29]	2018	FW-DBA algorithm is designed to adjust ONU bandwidth on multiple wavelengths by the offered load.	Frame reordering is not considered.
[30]	2018	SCAP scheme reports better bandwidth utilization over WF-DWBA.	The descending arrangement of ONU demands causes higher delays for ONUs with low loads.
[33]	2022	DWBA-FRA algorithm lowers the number of ONUs facing out-of-order frames than SCAP.	Not applicable for O-RAN environment.
[34]	2022	ONUs are grouped according to the load.	Not applicable for O-RAN.
[35]	2023	Channel bonding is performed considering load balancing and frame reordering delay reduction.	Multiple service groups are not considered.
This paper		A novel upstream DWBA scheme along with multi-OLT PON-based fronthaul for C-RAN is designed considering the channel bonding constraints properly. The load balancing is done by defining the same frame limit over multiple wavelengths. Consequently, the transmission overhead due to the extra guard time usage for an ONU transmitting on multiple wavelengths is reduced. Furthermore, the frame resequencing delay is also reduced and the additional delay due to non-fragmentable Ethernet frames is controlled.	

frequency bands and combine them into a single transmission path.

In conclusion of the section, it could be said that the proposed architecture has several advanced features compared to the referred existing architectures. TDM-PON met the 5G fronthaul delay requirement through an additional cooperative interface [18], [19], [20], [21]. Mobile scheduling information has to be sent 4 ms before upstream transmission from the user through the interface which is troublesome in mini-slot-based 5G NR. On the other hand, the proposed architecture utilizes the existing PON structure without the need for an additional interface. It can sustain mini-slot-based 5G NR on top of existing data services. The network is easily scalable to promote multiple services by cost-effectively extending the number of OLTs. Existing TWDM-PON-based solutions provide low bandwidth utilization in low-loaded ONUs [22] and do not address the channel bonding constrains well [24]. While the proposed architecture provides high bandwidth utilization and energy saving by sharing access to the G-class ONU structure. In the proposed P-class ONU structure, 5G service can leverage dynamic channel bonding to achieve the peak rate if necessary. As there are multiple OLTs in the network sharing MPCP and DBA poling table, an active OLT can restore service of other faulty OLTs and emergency services like 5G can persist uninterrupted. Therefore, the proposed network provides additional features of service protection and restoration. Finally, multiple services confirm the convergence in the network, and the system stability is provided in the result section.

IV. PROPOSED WAVELENGTH AND BANDWIDTH ALLOCATION

Resource allocation is a vital issue in multi-wavelength lane NG-PON. An efficient wavelength and bandwidth allocation scheme can make high utilization of network resources. We

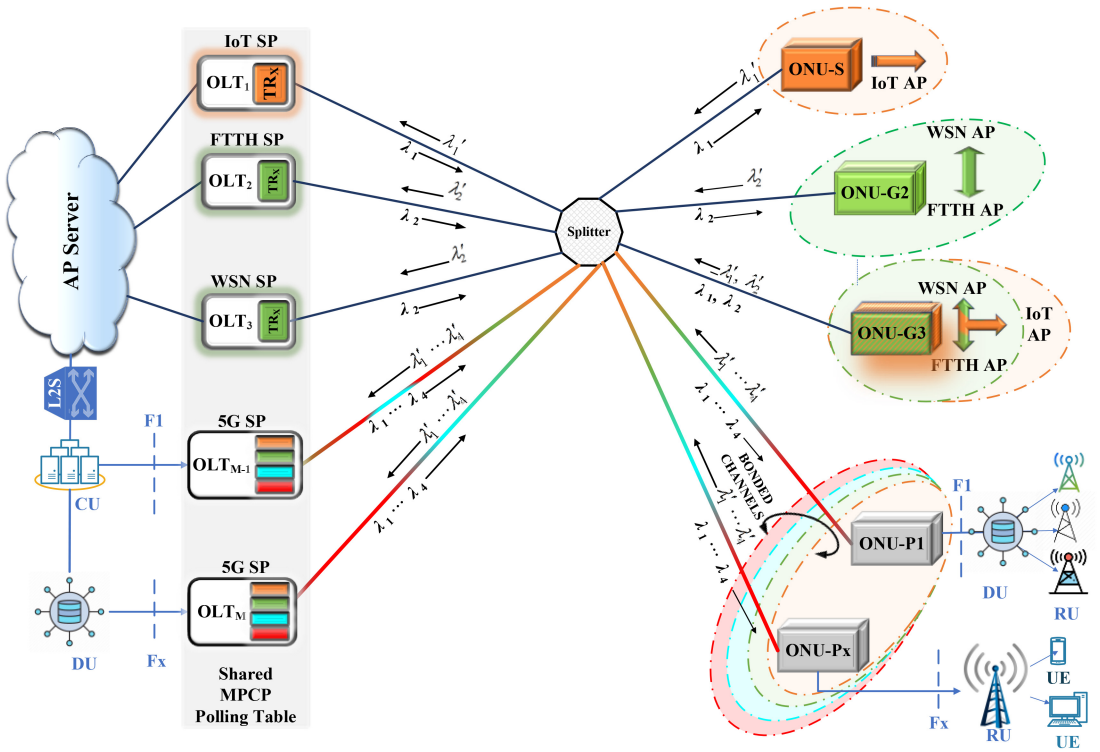

FIGURE 1. Network architecture of the proposed multi-OLT multi-lane PON-based OAN.

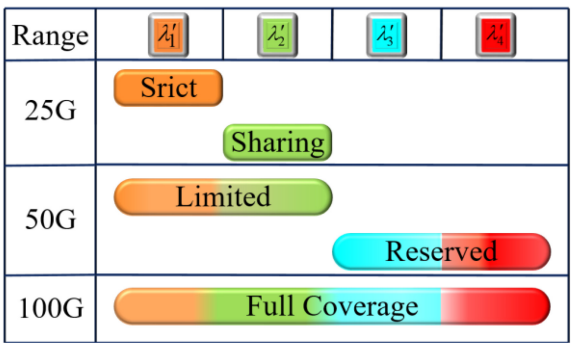

FIGURE 2. Access categories and ONU range.

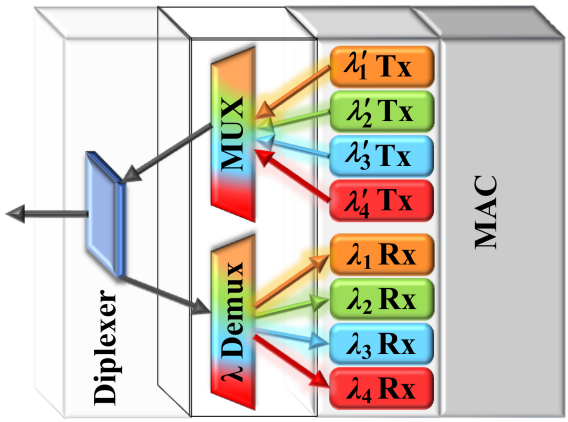

FIGURE 3. The proposed platinum-class ONU structure.

propose an NG-PON network having multiple OLTs. A novel scheme named ACP-2D is designed to cope in the multi-OLT multi-lane 100Gb/s PON environment. Fixed optics is used here to endorse parallel WDM in broadcast fashion from scalability and low-cost perspectives [38]. Fixed colors are used on per service class silver and gold. 100G ONUs can leverage service on multiple wavelengths using channel bonding. This makes wavelength assignments flexible using a fixed and dynamic variation. High bandwidth utilization can be achieved by assigning higher rate ONUs on multiple wavelength channels for load balancing and lowering the overhead due to guard band by assigning simple service class ONUs on a single channel. This situation makes low-loaded ONUs reside in a smaller number of wavelengths which also reduces frame size mismatch with assigned bandwidth.

The P-class is to be arranged in ascending order of bandwidth demand for channel bonding. The remaining bandwidth demand is provided possibly in the same wavelength channel previously assigned to avoid frame reordering problems. The principle of the scheme can be summarized as follows. Firstly, the wavelength of each service class is fixed. Only higher-priority services like 5G can extend wavelength usage by channel bonding. Secondly, low-priority simple class ONUs are to reside on a single wavelength lane which reduces frame size mismatch. Thirdly, top priority highly loaded ONUs are given the chance of channel bonding to achieve the full rate of 100G. This situation leverages load

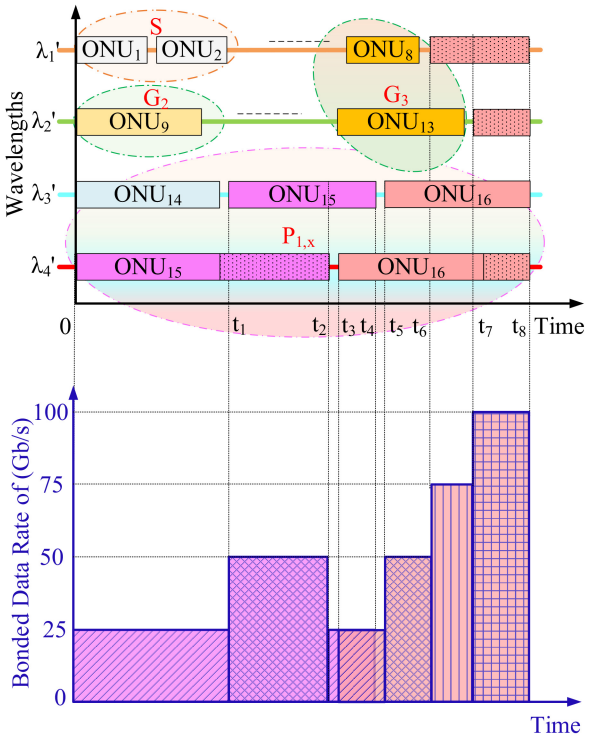

FIGURE 4. ACP-2D explanation.

balancing. Fourthly, each ONU utilizes up to a predefined maximum bandwidth in the assigned wavelength for fairness and saves excess bandwidth if any. This is one dimension of the scheme. Finally, the higher rate ONUs extend bandwidth to the excess part of other wavelengths by bonding process which is the second dimension of the scheme.

Fig. 4 shows a possible allocation mode for the proposed ACP-2D scheme. The 1st wavelength lane poses a total of nine subscribed ONUs, eight of them are from S-class and the remaining one is from G3. This ONU G3 receives three services in total, one from the 1st lane and the other two from the 2nd lane. A total of five subscriber ONUs are there in the 2nd lane, all from G-class. The 3rd and 4th lanes are exclusively reserved for P-class, i.e., 5G ONUs. These ONUs can partake in excess bandwidth in the other two lanes through channel bonding if necessary. The down part of the figure shows how the P-class ONUs partake higher rates by dynamic channel bonding. Table 2 shows the list of useful notations for the ACP-2D scheme. Table 3 shows the procedure to calculate the number of ONUs per wavelength lane. Actually, the total number of ONUs (N_k) in the k'th lane not only depends on the subscriber ONUs (N^X) but also on the ONUs of P-class, $N^P_{k,bon}$ that came to this lane for channel bonding. The example in this table shows from Fig. 4 how to calculate the number of ONUs that need bonding to the next wavelength.

Pseudocode of the ACP-2D scheme is expressed in Algorithm 1. Bandwidth on each wavelength is assigned (line 1). Bandwidths on the 1st and 2nd lanes are divided

TABLE 2. List of notations.

Notation	Description
K	Number of wavelengths
k	The wavelength identifier $k = 1, 2, ..., K$
M	Total set of OLTs or SPs (IoT, FTTH, WSN, and 5G)
N	Total set of ONUs
N^X	The set of ONUs in X (S, G2, G3, P)-service class
N_k	The set of ONUs in k'th wavelength
N^P_k	The set of P-class ONUs that resides in in the k'th wavelength only
$N^P_{k,bon}$	The set of P-class ONUs that needs bonding in the k'th wavelength
BW_k	The bandwidth of k'th wavelength
$BW^M_{k,\max}$	The maximum upstream bandwidth per ONU toward SP-M at k'th wavelength
BW^x_k	The bandwidth of the x'th ONU of X-class at k'th wavelength
$BW_{k,exs}$	Excess bandwidth at k'th wavelength
$BW^x_{k,req}$	The bandwidth request of x'th ONU of X-class in k'th wavelength
$BW^p_{k,rbr}$	The remaining bandwidth request of p'th P-class ONU in k'th wavelength

among constituent ONUs according to bandwidth agreement (lines 3-5). P-class ONUs are to be assigned in the 3rd and 4th lanes (lines 6-7). The remaining bandwidth requests are to be calculated (line 8). Excess bandwidth of the wavelengths is to be calculated (line 9). Finally, remaining bandwidth requests are to be satisfied for P-class ONUs through channel bonding to other lanes that have excess bandwidths. The first three steps can be grouped as Dimension-I and the last step as Dimension-II.

The Dimension-I of Algorithm 1 is run for all wavelength lanes (line 1). For the 1st and 2nd lanes (lines 3-5), bandwidth assignment could be expressed through (1) to (13). The total bandwidth of 1st lane ($k = 1$) is expressed as

$$BW_1 = BW^{IoT}_{1,\max} \times \left(N^S + N^{G3}\right), \tag{1}$$

where $N^S$and $N^{G3}$are the number of ONUs in S and $G3$ classes, respectively. The maximum bandwidth per ONU in IoT service is defined as

$$BW^{IoT}_{1,\max} = BW_1 / \left(N^S + N^{G3}\right) \tag{2}$$

The assigned upstream bandwidth of the S-class or G-class ONU for IoT services in the 1st lane is determined on the respected bandwidth request value as

$$BW^{s,g}_1 = \begin{cases} BW^{IoT}_{1,\max}, & BW^{s,g}_{1,req} \geq BW^{IoT}_{1,\max} \\ BW^{s,g}_{1,req}, & BW^{s,g}_{1,req} < BW^{IoT}_{1,\max}, \end{cases} \tag{3}$$

where $BW^{s,g}_{1,req}$ is the requested bandwidth for s or g^{th} ONU in the corresponding S-$class$ or G-class.

Finally, the excess bandwidth on the 1st lane is calculated as

$$BW_{1,exs} = BW_1 - \sum_{s \in S} BW^s_1 - \sum_{g \in G3} BW^g_1. \tag{4}$$

TABLE 3. Number of ONUs per wavelength lane calculation procedure.

Parameter	Calculation Procedure
Total set of ONUs per wavelength N_k	$N_1 = N^S + N^{G3} + N^P_{1,bon}$ $N_2 = N^{G2} + N^{G3} + N^P_{2,bon}$ $N_3 = N^P = N^P_3 + N^P_{4,bon}$ $N_4 = N^P_{4,bon} = N^P_4 + N^P_{1,bon}$
Total set of bonded ONUs per wavelength $N^P_{k,bon}$	$N^P_{4,bon} = N^P - N^P_3 = N^P_4 + N^P_{1,bon}$ $N^P_{1,bon} = N^P_{4,bon} - N^P_4 = N^P_1 + N^P_{2,bon}$ $N^P_{2,bon} = \begin{cases} N^P_{1,bon} - N^P_1 & \text{if } BW_{1,exs} \geq \sum_{i \in N^P_1} BW^i_{1,rbr} \\ N^P_{1,bon} & \text{else} \end{cases}$
Total P-Class ONU N^P	$N^P = N^P_3 + N^P_{4,bon}$ $= N^P_3 + N^P_4 + N^P_1 + N^P_{2,bon}$ $\left(\because N^P_{2,bon} \subseteq N^P_{1,bon} \subseteq N^P_{4,bon}\right)$
Total set of ONUs N	$N = N_1 \cup N_2 \cup N_3 \cup N_4$ $= \sum_{x \in X} N^x = N^S + N^{G2} + N^{G3} + N^P$
Example	$N_3 = N^P = 3,\ N^P_3 = 1$ $N^P_{4,bon} = N^P - N^P_3 = 3 - 1 = 2$ $N^P_{1,bon} = N^P_{4,bon} - N^P_4 = 2 - 1 = 1$ $N^P_{2,bon} = N^P_{1,bon} = 1$ as $BW_{1,exs} < \sum_{i \in N^P_1} BW^i_{1,rbr}$

The total bandwidth of 2nd lane is divided to 2nd generation and 3rd generation G-class ONUs as follows:

$$BW_2 = BW^G_{2,\max} \times \left(N^{G2} + N^{G3}\right), \tag{5}$$

where N^{G2} is the number of ONUs in the $G2$-class.

The maximum bandwidth per ONU in the 2nd lane is defined as

$$BW^G_{2,\max} = BW_2 / \left(N^{G2} + N^{G3}\right). \tag{6}$$

Again, the maximum bandwidth is shared by two SP groups like FTTH and WSN as follows:

$$BW^G_{2,\max} = BW^{FTTH}_{2,\max} + BW^{WSN}_{2,\max}, \tag{7}$$

where $BW^{FTTH}_{2,\max}$ and $BW^{WSN}_{2,\max}$ are the maximum bandwidth per ONU for FTTH and WSN groups, respectively.

The maximum bandwidth per ONU of the 2nd lane is thus divided towards FTTH and WSN SPs. FTTH achievesγ percent of the total bandwidth through service level agreement (SLA) as follows:

$$BW^{FTTH}_{2,\max} = \gamma BW^G_{2,\max} = \gamma BW_2 / \left(N^{G2} + N^{G3}\right) \tag{8}$$

The rest of the maximum bandwidth is calculated for WSN as follows:

$$BW^{WSN}_{2,\max} = (1-\gamma) BW^G_{2,\max} = (1-\gamma) BW_2 / \left(N^{G2} + N^{G3}\right). \tag{9}$$

The total assigned bandwidth for g'th G-class ONU is calculated as

$$BW^g_2 = BW^f_2 + BW^w_2, \tag{10}$$

where BW^f_2 and BW^w_2 are individually assigned bandwidths to FTTH and WSN, respectively.

The upstream bandwidth per ONU assigned for FTTH SP is determined as

$$BW^f_2 = \begin{cases} BW^{FTTH}_{2,\max}, & BW^f_{2,req} \geq BW^{FTTH}_{2,\max} \\ BW^f_{2,req}, & BW^f_{2,req} < BW^{FTTH}_{2,\max}, \end{cases} \tag{11}$$

where $BW^f_{2,req}$ is the value of the requested bandwidth of f'th ONU of FTTH SP.

The upstream bandwidth per ONU assigned for WSN SP is defined as

$$BW^w_2 = \begin{cases} BW^{WSN}_{2,\max}, & BW^w_{2,req} \geq BW^{WSN}_{2,\max} \\ BW^w_{2,req}, & BW^w_{2,req} < BW^{WSN}_{2,\max}, \end{cases} \tag{12}$$

where $BW^w_{2,req}$ is the requested bandwidth of w'th ONU of WSN SP.

At last excess bandwidth is calculated for 2nd wavelength lane as

$$BW_{2,exs} = BW_2 - \sum_{f \in FTTH} BW^f_2 - \sum_{w \in WSN} BW^w_2. \tag{13}$$

Bandwidth on 3rd and 4th lanes (lines 7-11) is assigned as (14) to (27). The bandwidth of the 3rd lane, BW_3 is assigned to P-class ONUs (BW^P_3), and the excess part $BW_{3,exs}$ is reserved for re-distribution as

$$BW_3 = BW^P_3 + BW_{3,exs}. \tag{14}$$

The maximum bandwidth per P-class ONU on the 3rd lane can be expressed as

$$BW^P_{3,\max} = BW_3 / N^P, \tag{15}$$

where N^P is the number of total P-class ONUs.

The bandwidth assigned to each P-class ONU on the 3rd lane can be defined as

$$BW^p_3 = \begin{cases} BW^P_{3,\max}, & BW^p_{3,req} > BW^P_{3,\max} \\ BW^p_{3,req}, & BW^p_{3,req} \leq BW^P_{3,\max}, \end{cases} \tag{16}$$

where $BW^p_{3,req}$ is the requested bandwidth of p'th P-class ONU.

The remaining bandwidth request on the 3rd lane of p'th P-class ONU is calculated as follows:

$$BW^p_{3,rbr} = \begin{cases} BW^p_{3,req} - BW^P_{3,\max}, & BW^p_{3,req} > BW^P_{3,\max} \\ 0, & BW^p_{3,req} \leq BW^P_{3,\max}. \end{cases} \tag{17}$$

Algorithm 1 ACP-2D Procedure

Dimension-I: Bandwidth Assignment per Predefined Wavelength

1: for $(k = 1 : K)$ do
2: for $(n \in N_k)$ do
3: if $k \leq 2$ then
4: Assign $BW^M_{k,\max}$ to constituent ONU class
5: Calculate total excess bandwidth $BW_{k,exs}$
6: else
7: Assign bandwidth BW^p_k
8: Calculate remaining requests $BW^p_{k,rbr}$
9: Calculate excess bandwidth $BW^p_{k,exs}$
10: Update N^P_k, $N^P_{k+1,bon}$
11: Calculate total excess bandwidth $BW_{k,exs}$
12: end if
13: end for
14: end for

Dimension -II: Dynamic Channel Bonding

1: if $\sum_{j\in K} BW_{j,exs} \geq \sum_{i\in P} BW^i_{4,rbr}$ then
2: Use max-min fairness:
3: for $(k = 1 : K)$ do
4: for $\left(p \in N^P_{k,bon}\right)$ do
5: Assign $BW^p_{k,rbr}$ from $BW_{k,exs}$
6: Update $BW^p_{k+1,rbr}$, BW^p_k, and $N^P_{k+1,bon}$
7: end for
8: end for
9: else
10: Use proportional fairness:
11: for $(k = 1 : K)$ do
12: for $\left(p \in N^P_{k,bon}\right)$ do
13: Assign $BW^p_{k,rbr}$ from $BW_{k,exs}$
14: Update $BW^p_{k+1,rbr}$, BW^p_k, and $N^P_{k+1,bon}$
15: end for
16: end for
17: end if

The unutilized excess amount of bandwidth of p'th P-class ONU on the 3rd lane is calculated as

$$BW^p_{3,exs} = \begin{cases} 0, & BW^p_{3,req} > BW^P_{3,\max} \\ BW^P_{3,\max} - BW^p_{3,req}, & BW^p_{3,req} \leq BW^P_{3,\max}. \end{cases} \quad (18)$$

The number of ONUs that need bonding on the next 4th lane, $N^P_{4,bon}$ is updated according to the requested bandwidth as

$$\text{Update} \begin{cases} N^P_{4,bon} = N^P_{4,bon} + \{p\}, & BW^p_{3,req} > BW^P_{3,\max} \\ N^P_3 = N^P_3 + \{p\}, & BW^p_{3,req} \leq BW^P_{3,\max}, \end{cases} \quad (19)$$

where N^P_3 is the number of ONUs that only need bandwidth at the 3rd lane.

Finally, for the 3rd lane excess bandwidth is determined as

$$\begin{aligned} BW_{3,exs} &= \sum_{p\in N^P} BW^p_{3,exs} \\ &= BW_3 - \sum_{i\in N^P_3} BW^i_3 - \sum_{j\in N^P_{4,bon}} BW^j_3. \end{aligned} \quad (20)$$

The bandwidth of the 4th lane, BW_4 is distributed to P-class ONUs (BW^P_4) at this lane, and the excess part $BW_{4,exs}$(which is reserved for re-distribution) is calculated as

$$BW_4 = BW^P_4 + BW_{4,exs}. \quad (21)$$

The maximum bandwidth per P-ONU in the 4th lane is expressed as

$$BW^P_{4,\max} = BW_4/N^P. \quad (22)$$

The remaining bandwidth request on the 4th lane is updated to $BW^p_{4,rbr} = BW^p_{3,rbr}$. Then bandwidth is assigned to P-class ONUs as

$$BW^p_4 = \begin{cases} BW^P_{4,\max}, & BW^p_{4,rbr} > BW^P_{4,\max} \\ BW^p_{4,rbr}, & BW^p_{4,rbr} \leq BW^P_{4,\max}. \end{cases} \quad (23)$$

The remaining bandwidth request gets the final value as

$$BW^p_{4,rbr} = \begin{cases} BW^p_{4,rbr} - BW^P_{4,\max}, & BW^p_{4,rbr} > BW^P_{4,\max} \\ 0, & BW^p_{4,rbr} \leq BW^P_{4,\max}. \end{cases} \quad (24)$$

The excess bandwidth per P-class ONU is obtained as

$$BW^p_{4,exs} = \begin{cases} 0, & BW^p_{4,rbr} > BW^P_{4,\max} \\ BW^P_{4,\max} - BW^p_{4,rbr}, & BW^p_{4,rbr} \leq BW^P_{4,\max}. \end{cases} \quad (25)$$

The number of ONUs that need bonding on the next lane $(k = 1)$ is updated as

$$\text{Update} \begin{cases} N^P_{1,bon} = N^P_{1,bon} + \{p\}, & BW^p_{4,rbr} > BW^P_{4,\max} \\ N^P_4 = N^P_4 + \{p\}, & BW^p_{4,rbr} \leq BW^P_{4,\max}. \end{cases} \quad (26)$$

The total excess bandwidth on the 4th lane is found from the following equation:

$$BW_{4,exs} = \sum_{p\in N^P} BW^p_{4,exs} = BW_4 - \sum_{i\in N^P_4} BW^i_4 - \sum_{j\in N^P_{1,bon}} BW^j_4. \quad (27)$$

Important equations for regular bandwidth allocation on corresponding wavelengths according to Dimension-I of Algorithm-1 are summarized in Table 4.

TABLE 4. Summary of the important equations.

Parameter	Equation	Eq. no.
BW_k	$BW_1 = BW^{IoT}_{1,\max} \times \left(N^S + N^{G3}\right)$	1
	$BW_2 = BW^{G}_{2,\max} \times \left(N^{G2} + N^{G3}\right)$	5
	$BW_3 = BW^{P}_{3} + BW_{3,exs}$	14
	$BW_4 = BW^{P}_{4} + BW_{4,exs}$	21
$BW^M_{k,\max}$	$BW^{IoT}_{1,\max} = BW_1 \Big/ \left(N^S + N^{G3}\right)$	2
	$BW^{FTTH}_{2,\max} = \gamma BW_2 \Big/ \left(N^{G2} + N^{G3}\right)$	8
	$BW^{WSN}_{2,\max} = (1-\gamma) BW_2 \Big/ \left(N^{G2} + N^{G3}\right)$	9
	$BW^{P}_{3,\max} = BW_3 \Big/ N^P$	15
	$BW^{P}_{4,\max} = BW_4 \Big/ N^P$	22
BW^x_k	$BW^{s,g}_1 = \begin{cases} BW^{IoT}_{1,\max}, & BW^{s,g}_{1,req} \geq BW^{IoT}_{1,\max} \\ BW^{s,g}_{1,req}, & BW^{s,g}_{1,req} < BW^{IoT}_{1,\max} \end{cases}$	3
	$BW^{g}_2 = BW^{f}_2 + BW^{w}_2$	10
	$BW^{p}_3 = \begin{cases} BW^{P}_{3,\max}, & BW^{p}_{3,req} > BW^{P}_{3,\max} \\ BW^{p}_{3,req}, & BW^{p}_{3,req} \leq BW^{P}_{3,\max} \end{cases}$	16
	$BW^{p}_4 = \begin{cases} BW^{P}_{4,\max}, & BW^{p}_{4,rbr} > BW^{P}_{4,\max} \\ BW^{p}_{4,rbr}, & BW^{p}_{4,rbr} \leq BW^{P}_{4,\max} \end{cases}$	23

Algorithm 2a Max-Min Fairness Bonding for $\lambda_{k\{3,4\}}$

```
while (BW_{k,exs} ≠ 0) do
  for (p ∈ N^P_{4,bon}) do
    if (BW^p_{4,rbr} ≤ BW_{k,exs}) then
      BW^p_k = BW^p_k + BW^p_{4,rbr}
      BW_{k,exs} = BW_{k,exs} − BW^p_{4,rbr}
      N^P_{k+1,bon} = N^P_{4,bon} − {p}
      BW^p_{k+1,rbr} = 0
    else
      BW^p_k = BW^p_k + BW_{k,exs}
      BW^p_{k+1,rbr} = BW^p_{4,rbr} − BW_{k,exs}
      N^P_{k+1,bon} = N^P_{k+1,bon}
      BW_{k,exs} = 0
    end if
  end for
end while
```

Algorithm 2b Max-Min Fairness Bonding for $\lambda_{k\{1,2\}}$

```
while (BW_{k,exs} ≠ 0) do
  for (p ∈ N^P_{k,bon}) do
  if (BW^p_{k,rbr} ≤ BW_{k,exs}) then
    BW^p_k = BW^p_{k,rbr}
    BW^p_{k+1,rbr} = 0
    N^P_{k+1,bon} = N^P_{k,bon} − {p}
      BW_{k,exs} = BW_{k,exs} − BW^p_{k,rbr}
    else
    BW^p_k = BW_{k,exs}
    BW^p_{k+1,rbr} = BW^p_{k,rbr} − BW_{k,exs}
    N^P_{k+1,bon} = N^P_{k+1,bon}
    BW_{k,exs} = 0
      end if
    end for
end while
```

In the case $k = K, k+1 \rightarrow 1$. In the case $k = 2$, $N^P_{k+1,bon} \rightarrow 0$, and $BW^p_{k+1,rbr} \rightarrow 0$.

The Dimension-II of Algorithm 1 is run due to the channel bonding of P-class ONUs. Remaining bandwidth requests can be allocated serially to ONUs during bonding with ascending demand if the sum of total excess bandwidth of all lanes is higher or equal to the sum of remaining bandwidth requests (lines 1-6). Therefore, on condition $\sum_{j\in K} BW_{j,exs} \geq \sum_{i\in P} BW^i_{4,rbr}$ (line 1), the max-min fairness process can be expressed as Algorithm 2a for the 3rd and 4th lanes. Then, the remaining 1st and 2nd lanes re-allocate the excess bandwidth by max-min fairness according to Algorithm 2b.

Remaining bandwidth requests can be allocated in proportional fairness to ONUs if the sum of the total excess bandwidth of all lanes is less than the requests (Algorithm 1, Dimension-II, line 9). Therefore, on condition ($\sum_{j\in K} BW_{j,exs} < \sum_{i\in P} BW^i_{4,rbr}$), the proportional fairness process (lines 11-14) can be expected. The process can be expressed as Algorithm 3a for the 3rd and 4th lanes. Then the remaining 1st and 2nd lanes re-allocate excess bandwidth by proportional fairness according to Algorithm 1. The sequences of the algorithms used in ACP-2D scheme are summarized as a flowchart in Fig. 5. The bandwidth allocation on each wavelength is performed according to Dimension-I of Algorithm 1. If some ONUs need channel bonding then Dimension-II of Algorithm 1 is executed. If the excess bandwidth of the network is enough for the remaining demand, then Algorithm 2a is executed otherwise Algorithm 2b is the choice.

The computational complexity of Dimension-I of Algorithm 1 can be stated as $O(K \times |N_k|)$. If channel bonding is needed, Dimension-II is executed with complexity $O(K \times |N^P_{k,bon}|)$. Here, the number of wavelengths, the number of ONUs in k'th wavelength, and the number of ONUs in P-class that need channel bonding are K, $|N_k|$, and $|N^P_{k,bon}|$, respectively. The first one is the constant variable which reduces the total computational complexities $O(K \times |N_k|) + O(K \times |N^P_{k,bon}|)$ to $O(|N_k|) + O(|N^P_{k,bon}|)$. The computational complexity will not affect the practical applicability of the proposed algorithm as the computed optimum solution is continuously applied until the network condition changes.

Algorithm 3a Proportional Fairness Bonding for $\lambda_{k\{3,4\}}$

$N^P_{k+1,bon} = N^P_{4,bon}$
for $\left(p \in N^P_{4,bon}\right)$ do
  $\Delta^p_k = BW^p_{4,rbr} / \sum_p BW^p_{4,rbr}$
  $BW^p_k = BW^p_k + BW_{k,exs} \times \Delta^p_k$
  $BW^p_{k+1,rbr} = BW^p_{4,rbr} - BW_{k,exs} \times \Delta^p_k$
  if $\left(BW^p_{k+1,rbr} \leq 0\right)$ then
    $N^P_{k+1,bon} = N^P_{4,bon} - \{p\}$
  end if
end for

Algorithm 3b Proportional Fairness Bonding for $\lambda_{k\{1,2\}}$

$N^P_{k+1,bon} = N^P_{k,bon}$
for $\left(p \in N^P_{k,bon}\right)$ do
  $\Delta^p_k = BW^p_{k,rbr} / \sum_p BW^p_{k,rbr}$
  $BW^p_k = BW_{k,exs} \times \Delta^p_k$
  $BW^p_{k+1,rbr} = BW^p_{k,rbr} - BW_{k,exs} \times \Delta^p_k$
if $\left(BW^p_{k+1,rbr} \leq 0\right)$ then
  $N^P_{k+1,bon} = N^P_{k,bon} - \{p\}$
  end if
end for In the case $k = K, k+1 \rightarrow 1$. In the case $k = 2$, $N^P_{k+1,bon} \rightarrow 0$, and $BW^p_{k+1,rbr} \rightarrow 0$.

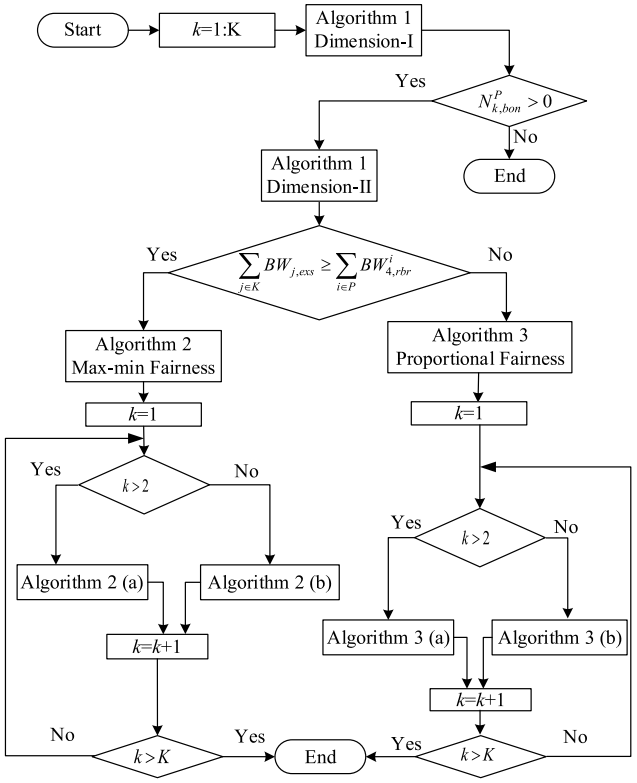

FIGURE 5. Flowchart of the algorithms.

In the concluding note of this section, it could be mentioned that the challenges involved in designing a DWBA in NG-EPON are – load balancing, transmission overhead management by reducing extra guard time, dropping frame resequencing delay, and allocating excess bandwidth on the same wavelength as much as possible due to non-fragmentable nature of Ethernet frames. None of the existing algorithms addresses all of them together. WF-DWBA [27] promotes load balance in the cost of lowering bandwidth utilization. FF-DWBA algorithm [28] increases bandwidth utilization without considering load fluctuation. FW-DBA does not consider frame reordering [29]. SCAP scheme is not good enough to low-load ONUs [30]. DWBA-FRA algorithm [33] and DWBA-RSO [35] do not consider service grouping. The proposed ACP-2D scheme in this paper overcomes all the above limitations.

V. SIMULATION RESULTS

The performance analysis of the multi-OLT multi-lane PON is justified by the simulation of a 100 Gb/s NG-EPON. MATLAB programming is used to make the simulating software. Upstream network performance is analyzed through delay, throughput, jitter, overhead-to-data ratio (ODR), and bandwidth utilization (BWU).

A. SIMULATION PARAMETERS

The network is supposed to have four OLTs occupied by four individual SPs like IoT, FTTH, WSN, and 5G fronthaul and sixteen ONUs in total. ONUs are grouped into service classes. There are eight ONUs in the *S*-class. Along with these ONUs, one G3 ONU receives IoT services in 1st lane. Self-similar traffic (SST) is generated to characterize these IoT services with a constant packet size of 317 bytes. To generate SST, the procedure is followed as described in [9]. Each ONU in this group is targeted to have 1 Gb/s of throughput each posing in total 0.90 load in the network. Four G2 ONUs and one G3 ONU receive G-class service, i.e., FTTH in conjugate with WSN sharing the 2nd wavelength lane. The traffic used for this purpose is SST with variable packet lengths (64-1518 bytes). The throughput target of this group is 10.2 Gb/s (=5.1×2) catering to a net load share of 0.102 in the 100 Gb/s network. Queue size is assumed unlimited as the target is to satisfy the 5G delay requirements through reliable transmission of the traffic. Three ONUs are consumed in the 5G subscriber group. Three ONUs generate traffic having a 1518-byte packet length with a constant interval of packet gap. They represent a single-sector cell site, a double-sector cell site, and a triple-sector cell site, respectively. They pose a total throughput target of 79.8 Gb/s by each of 13.3 Gb/s, 26.6 Gb/s, and 39.9 Gb/s, respectively. The throughput value of 13.3 Gb/s per sector is calculated based on wireless spectrum bandwidth of 100 MHz at 15 bits per sample in the uplink. The antenna considered is 4×4 MIMO. The calculation is done in reference to the 3GPP TR 38.816, Release 15 [38]. Fronthaul option 7.1 (Fx interface) is used to facilitate the

TABLE 5. ONU load distribution.

SP	Class	ONU Number	Throughput (Gb/s)	Load
IoT	S+G3	8+1	9	0.09
FTTH	G2+G3	4+1	5.1	0.102
WSN			5.1	
5G	P	3	79.8	0.798

TABLE 6. Simulation parameters.

Parameter	Value
Network capacity (C)	100 Gb/s
Wavelength (λ)	4
OLT (M)	4
ONU (N)	16
FTTH reservation (γ)	50%
IoT packet size	317 bytes
FTTH and WSN packet size	64-1518 bytes
5G packet size	1518 bytes
Simulation run time	2 sec
Cycle time (T)	36, 71, 125, 500 µsec
Guard time (T_{guard})	0.01µsec
Control message ($T_{GATE/REPORT}$)	64 bytes

TABLE 7. 5G mini-slot variation.

SCS	Mini-slot duration (µsec)		
	7 symbols	4 symbols	2 symbols
15 kHz	500	286	143
30kHz	250	143	71
60 kHz	125	71	36

network through advanced features like CoMP and enhanced inter-cell interference coordination (eICIC). This information is summarized in Table 5 and Table 6.

Orthogonal frequency division multiplexing (OFDM) waveform is utilized in 5G NR. It also uses a scalable numerology with different sub-carrier spacings (SCS) like 15, 30, and 60 kHz below 6 GHz, and 60 and 120 kHz above 6 GHz [26]. 4G long-term evolution (LTE) utilizes OFDM but with a fixed numerology of 15 kHz. The basic frame structure or scheduling cycle in a mobile network is known as the slot. In 4G LTE, one slot has a transmission time interval of 1 ms to transmit 14 OFDM symbols at 15 kHz SCS. In the 5G NR, SCS gets higher and decreases OFDM symbols to a value of 2, 4, and 7 in the specification of standard. Thereby, the time drastically decreases to transmit a mini-slot. For example, at 60 kHz SCS and 4 OFDM symbols, the time achievable for a mini-slot is 71 μsec which is helpful for ultra-low latency 5G services. Table 7 shows the mini-slot durations with variable SCS. In our simulation, we investigated mini-slots of 36, 71, 125, and 250 μsec.

B. DELAY AND JITTER PERFORMANCE

Average packet delay is supposed to be the time needed for a packet transfer which is a collection of transmission, propagation, queueing, and processing delays. Although the queue size is kept unlimited, the queueing delay effect is included in the results by introducing serial congestion of first-in first-out queues. This part describes the upstream delay of ONU classes toward individual SP groups. One SP resides in one OLT. *P*-class ONUs pose 0.798 net loads and exclusively seized 3rd and 4th lanes (0.50 of net capacity) to transmit upstream data to 5G SP. Delay results are found well through the ACP-2D algorithm as it poses channel bonding to excess bandwidth of other wavelengths for an extra 0.298 of load. This result is compared to the results obtained with that of ACP-1D which is the variant of ACP-2D without the channel bonding for the 5G service. The delays are compared with varying frame lengths and distances as shown in Fig. 6. It is shown in Fig. 6 (a) that for the ACP-2D scheme, a frame length of 36 μsec has a maximum delay of 161.362 μsec up to a distance of 20 km which is within 250 μsec, the delay requirements of successful 5G transmission. The frame of 71 μsec also shows satisfactory results of a maximum of 220.332 μsec up to 20 km. Frame 125 μsec touches the delay threshold limit of 250 μsec at 7 km. The delay increases with the increment of frame size. Frame size 250 μsec and higher seems unusable in the ACP-2D scheme designed for the open-access environment. In conclusion, ACP-2D can satisfy 5G delay constraints for mini-slots with reliable transmission (full throughput). While ACP-1D transmits with a bit higher delay but in a great data loss (discussed further in the throughput sub-section). It is shown in Fig. 6 (b) that the ACP-1D frame length of 36 μsec has a maximum delay of 165.854 μsec up to a distance of 20 km. A slot of 71 μsec also shows results of a maximum of 229.241 μsec up to 20 km. Frame 125 μsec touches the delay threshold limit of 250 μsec at a shorter distance of 5 km.

Delays for IoT, FTTH, and WSN are achieved through ACP-2D in μsec range. ITU considers network delay for voice applications in Recommendation G.114. This recommendation defines three bands of one-way delay as shown in Table 8. Especially for FTTH video, voice, and data, the delay achieved within the μsec range in our proposed scheme is quite good. Fig. 7 shows that at 20 km, the maximum delay of IoT service is found. As shown in Fig. 7, for 36 μsec, 71 μsec, 125 μsec, and 250 μsec frame lengths, the maximum delays of IoT are 206.583 μsec, 252.956 μsec, 337.298 μsec, and 520.79 μsec, respectively. Fig. 8 represents the average upstream delay towards FTTH SP to be within well inside Rec G.114. The minimum delay value is 159.757 μsec at a 1 km ONU distance near 36 μsec frame length while the maximum value is found at 20 km at the highest delay of 546.94 μsec at a frame length

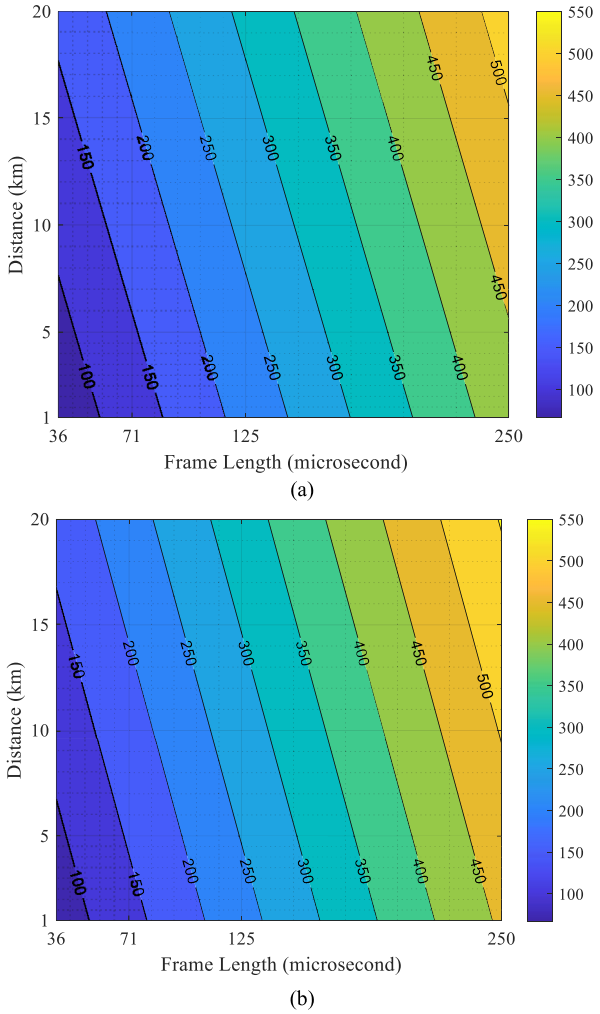

FIGURE 6. Average upstream delay (microsecond) to 5G fronthaul. (a) ACP-2D. (b) ACP-1D.

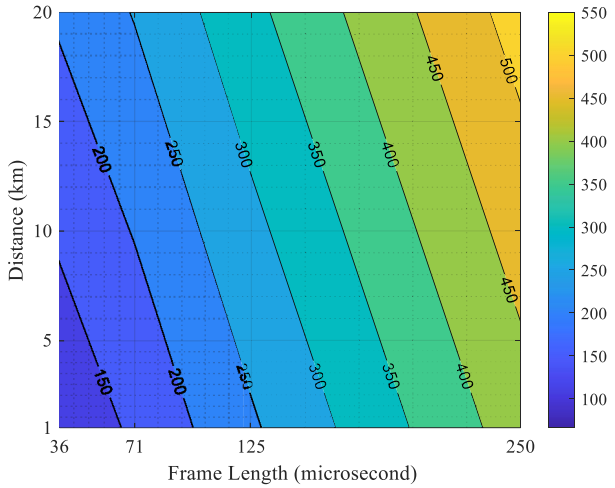

FIGURE 7. Average upstream delay (microsecond) to IoT.

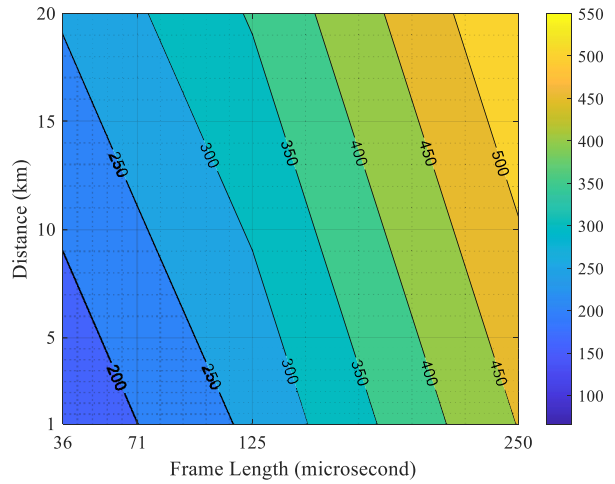

FIGURE 8. Average upstream delay (microsecond) to FTTH.

TABLE 8. Delay specification.

Range in msec.	Description
0~150	Acceptable for most user applications
150~400	Acceptable if administrators are aware of the transmission time and quality of user applications
Above 400	Unacceptable for general network planning

of 250 μsec. Fig. 9 depicts that at 20 km, the maximum upstream delays towards WSN SP for 36 μsec, 71 μsec, 125 μsec, and 250 μsec frame lengths are 259.636 μsec, 297.924 μsec, 362.046 μsec, and 560.139 μsec, respectively.

Jitter is the change in the time it takes for a data packet to travel across a network. The jitter performances of data towards all four SPs (IoT, FTTH, WSN, and 5G) are presented in Fig. 10. According to CISCO, the jitter should be below 30 msec for good video and voice quality. Fig. 10 shows that jitter to 5G service is increased slowly with frame length increase while IoT has the maximum swing. For 36 μsec, 71 μsec, 125 μsec, and 250 μsec frame lengths, the maximum jitters of IoT are 0.029 μsec, 0.057 μsec, 0.118 μsec, and 0.277 μsec, respectively. The lowest jitter of FTTH and WSN are shown to be 0.117 μsec and 0.123 μsec, respectively, at the frame length of 36 μsec. The highest jitter of FTTH and WSN are 0.260 μsec and 0.269 μsec, respectively, at the frame length of 250 μsec. For 36 μsec, 71 μsec, 125 μsec, and 250 μsec, the maximum jitters of 5G are 0.005 μsec, 0.011 μsec, 0.027 μsec, and 0.071 μsec, respectively.

C. THROUGHPUT PERFORMANCE

Throughput is determined as the ratio of transmitted data to transmission capacity. Fig. 11 shows throughput per *P*-class ONUs, i.e., subscribers of 5G SP. The target throughputs are shorted in ascending order for the ACP-2D algorithm. The ONU_{14}, ONU_{15}, and ONU_{16} generate data throughput of 13.3 Gb/s, 26.6 Gb/s, and 39.9 Gb/s, respectively. In total, they put a load of 79.8% on the network. As the

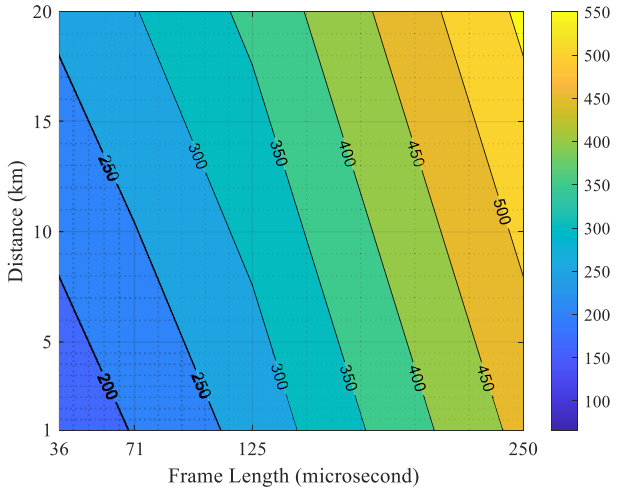

FIGURE 9. Average upstream delay (microsecond) to WSN.

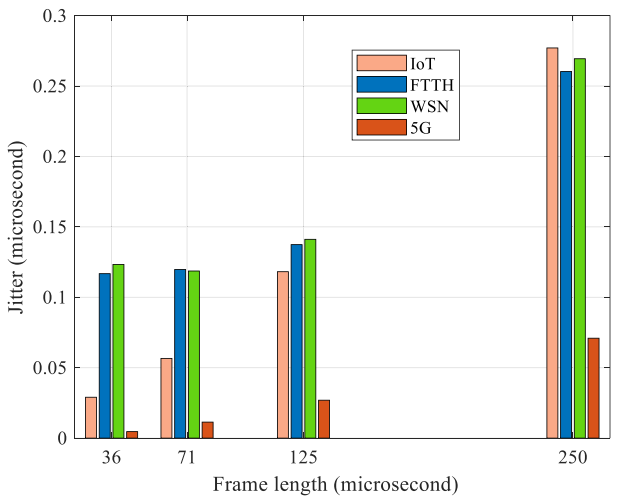

FIGURE 10. Jitter of four SPs at different frame lengths.

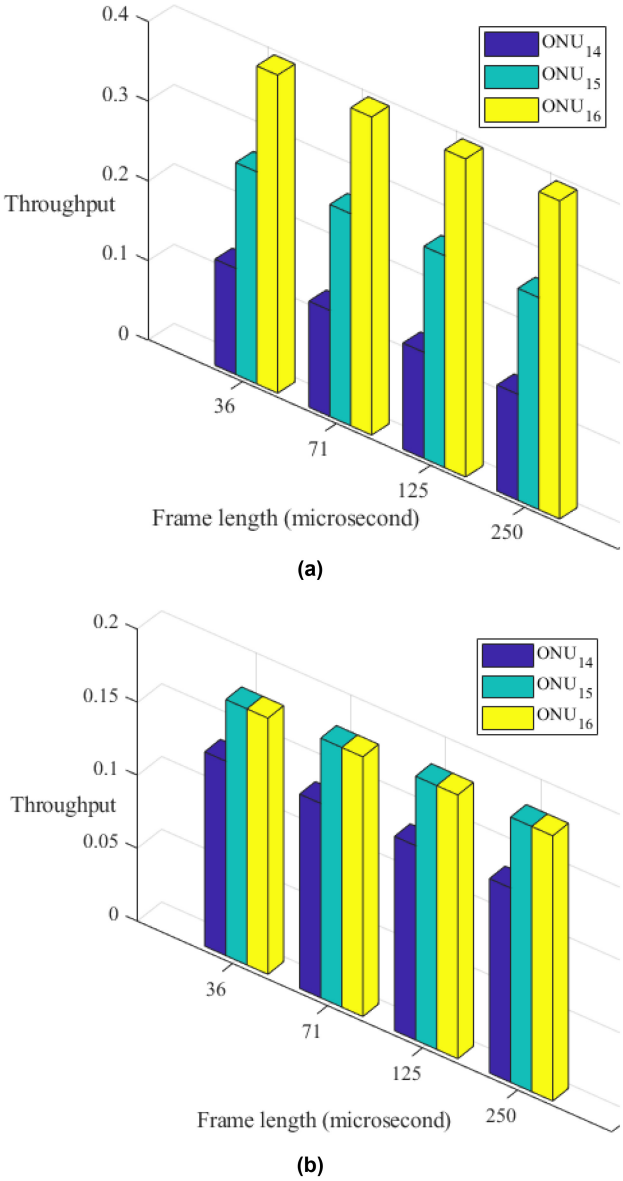

FIGURE 11. Throughput per ONU of 5G fronthaul SP. (a) ACP-2D. (b) ACP-1D.

reserved two-lane bandwidth (50 Gb/s) is not enough to satisfy the 5G load, the higher-rate ONUs need channel bonding with the rest of the two wavelengths. Load balance is achieved through this mechanism. As the total network load including 5G, IoT, and gold subscribers is within network capacity, there is enough bandwidth in the network to satisfy the 5G throughput targets. Fig. 11 (a) represents that ACP-2D works well in the access environment and achieves target throughput despite frame length variation. On the other hand, ACP-1D misses channel bonding. Fig. 11 (b) shows that for this variant only ONU_{14} almost achieves the desired throughput of 0.1331 per frame length while the other two ONUs restrict throughput to a low value so that the total achieved throughput is under 50%. For ONU_{15}, a maximum throughput of 0.182 is achieved at a frame length of 250 μsec and the lowest of 0.175 at 36 μsec frame. For ONU_{16}, maximum and minimum throughputs are restricted at the same values as ONU_{15}.

Individual throughput of the 1st wavelength lane is shown in Fig. 12 for the ACP-2D scheme. Eight *S*-class ONUs and one G3 ONU simply send upstream packets to the IoT SP. The rest of the excess bandwidth is utilized by *P*-class 5G subscribers for necessary channel bonding. Total throughput is slightly changing from frame length 36 μsec to 250 μsec as the amount of control packets is decreased in the network for higher frame length. The total posed IoT load is 0.091 on the network for this group which is achieved despite frame variation. The rest of the bandwidth is shared for channel bonding with 5G ONUs. At a frame length of 36 μsec, 5G ONUs achieved a throughput of 0.155 while at a frame length of 250 μsec, they get 0.156. The total throughput rise is from 0.2465 to 0.2478 at this lane. The throughput of the 2nd lane is presented in Fig. 13. G-class ONUs send data to FTTH

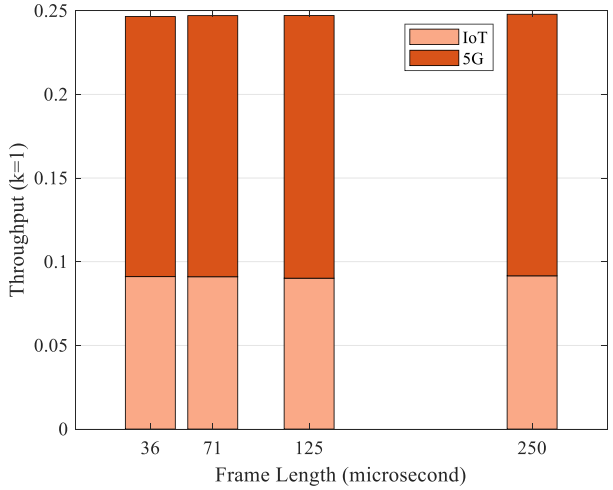

FIGURE 12. Throughput of the 1st lane (k=1).

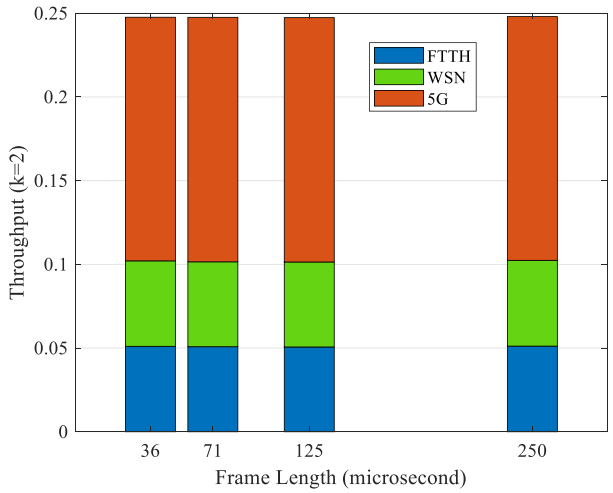

FIGURE 13. Throughput of the 2nd lane (k=2).

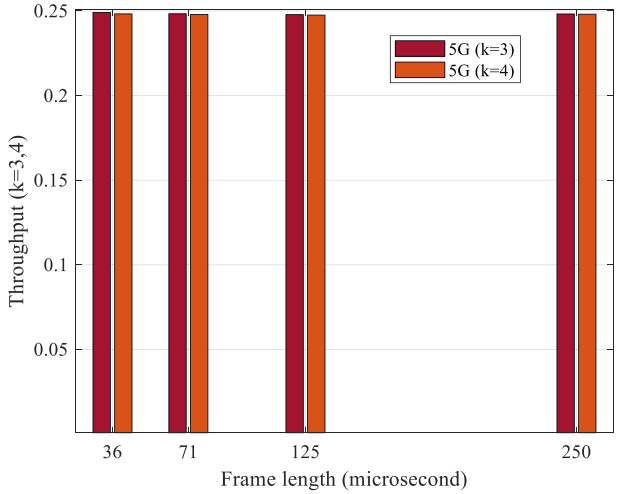

FIGURE 14. Throughput of the 3rd and 4th lane (k=3, 4).

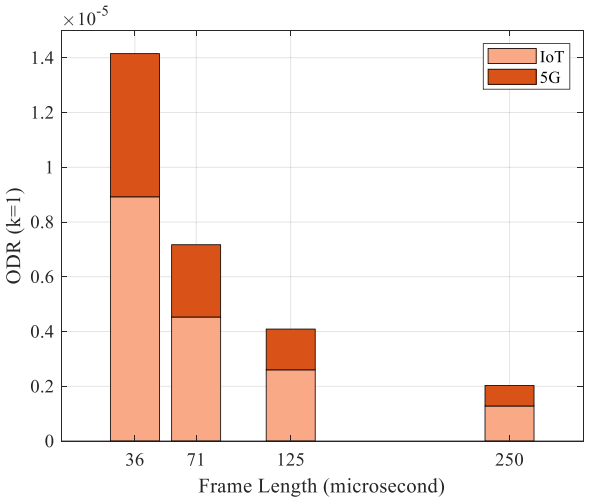

FIGURE 15. ODR of the 1st lane (k=1).

and WSN sharing this wavelength. To each of the ONUs, upstream packets are generated to fulfill the throughput target of 5.1 Gb/s per SP. A total of 10.2 Gb/s poses a load of 0.102 on the network. At each frame length, the rest of the excess bandwidth is used for channel bonding of 5G ONUs. The total minimum throughput achieved at frame length 36 μsec is 0.247 while the constituent groups FTTH, WSN, and 5G get 0.051, 0.051, and 0.145, respectively. Total maximum throughput is achieved at frame length 250 μsec as 0.248. Fig. 14 shows the throughputs of 5G ONUs in their exclusive 3rd and 4th wavelength lanes. On average, 5G ONUs achieve throughputs of 0.2483 in the 3rd lane and 0.2479 in the 4th lane.

D. ODR PERFORMANCE

ODR is the ratio of total overhead to transmitted data. ODR indicates whether the overhead used in the network is very high or not. Low ODR is an indication of good network performance. The increase in the frame length decreases the ODR drastically. Always frame length increment is not a solution as there is a tradeoff between delay and ODR. Fig. 15 shows the ODR of 1st lane through its constituent classes like IoT and 5G. For 36 μsec, 71 μsec, 125 μsec, and 250 μsec frame lengths, the ODR of IoT ONUs are 8.92×10^{-6}, 4.53×10^{-6}, 2.60×10^{-6}, and 1.28×10^{-6}, respectively. At the same frame sequence, the 5G ONUs create ODR of 5.23×10^{-6}, 2.64×10^{-6}, 1.49×10^{-6}, and 7.49×10^{-7}, respectively. Fig. 16 shows the ODR of 2nd lane through its constituent classes like gold and 5G. For 36 μsec, 71 μsec, 125 μsec, and 250 μsec frame lengths, the ODR of Gold ONUs are 5.31×10^{-6}, 2.71×10^{-6}, 1.54×10^{-6}, and 7.62×10^{-7}, respectively. At the same frame sequence, the 5G ONUs create ODR of 3.72×10^{-6}, 1.88×10^{-6}, 1.07×10^{-6}, and 5.36×10^{-7}, respectively. Fig. 17 shows the ODR of 3rd and 4th lanes for 5G services. For ascending the frame order, the 5G ODRs at the 3rd lane are 8.16×10^{-7}, 4.15×10^{-7}, 2.36×10^{-7}, and 1.18×10^{-7}, respectively. Finally, 4th lane ODR values of

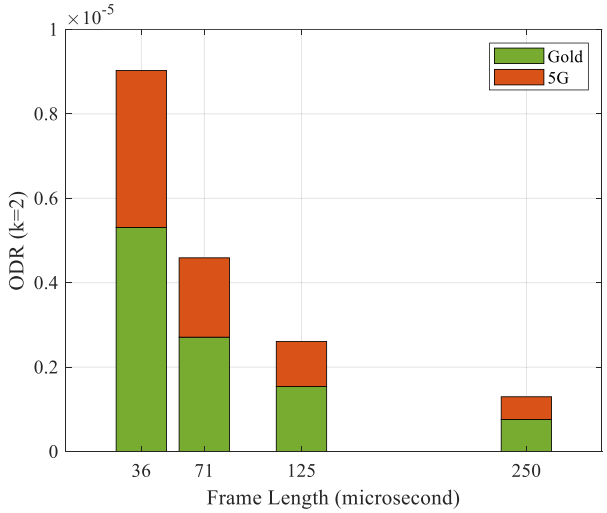

FIGURE 16. ODR of the 2nd lane (k=2).

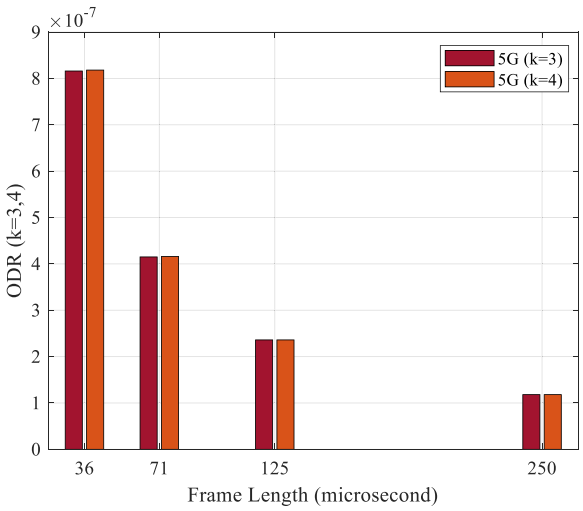

FIGURE 17. ODR of the 3rd and 4th lanes (k=3, 4).

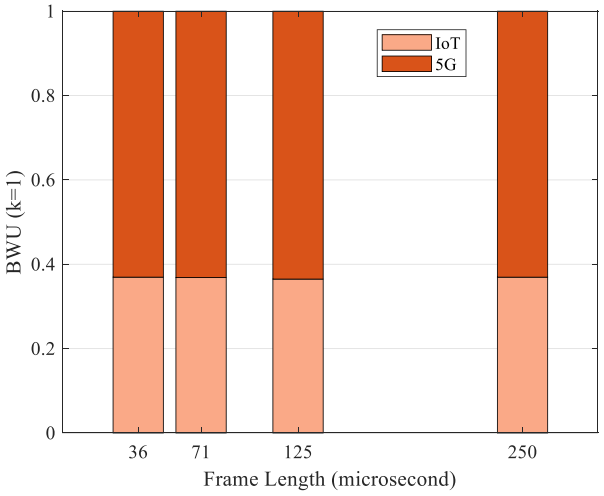

FIGURE 18. BWU of the 1st lane (k=1).

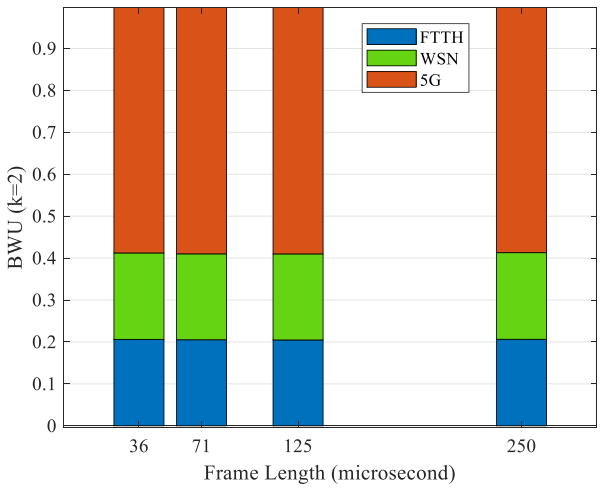

FIGURE 19. BWU of the 2nd lane (k=2).

5G are 8.18×10^{-7}, 4.16×10^{-7}, 2.36×10^{-7}, and 1.18×10^{-7}, respectively.

E. BWU PERFORMANCE

BWU is the amount of bandwidth consumed on a network and the breakdown of its composite traffic. BWU is determined as the ratio of transmitted data to the sum of the total control frame and transmitted data. Fig. 18 shows the BWU of the 1st lane, i.e., the amount of bandwidth consumed on this lane and the breakdown of its composite traffic IoT and 5G. Channel bonding of 5G ONU does not pose a huge amount of control frame, which is why the BWU is achieved 0.999. BWU for IoT and 5G are varied a little out of frame lengths and their average is 0.368 and 0.631, respectively. Fig. 19 shows a breakdown of bandwidth consumed on the 2nd lane to the composite traffic of FTTH, WSN, and 5G. BWU is almost unchanged from that of frame length. Average value of BWU for FTTH, WSN, and 5G are 0.205, 0.205, and 0.589, respectively. The total average BWU is achieved at 0.999. Fig. 20 shows the BWU of the 3rd and 4th lanes, i.e., kept exclusively for 5G services. BWU for 5G service is 0.999 for both of the lanes. The rest of the BWU is for the control frames.

In concluding notes of this section, it could be said that the proposed ACP-2D scheme successfully transmitted the desired throughput of 0.798 satisfying the 5G delay threshold of 250 μsec up to a mini-slot length of 125 μsec while maintaining other ongoing access services on the condition that the network capacity is enough to accommodate the total of all services. The ODR is low enough to achieve 99.9% BWU. Jitter is also in the tolerable range. Therefore, the proposed scheme provides performance stability.

VI. CONCLUSION

Radio access is paving an evolution path from distributed RAN to C-RAN to v-RAN and finally to O-RAN. This opens to vendors and multiple services further promoting

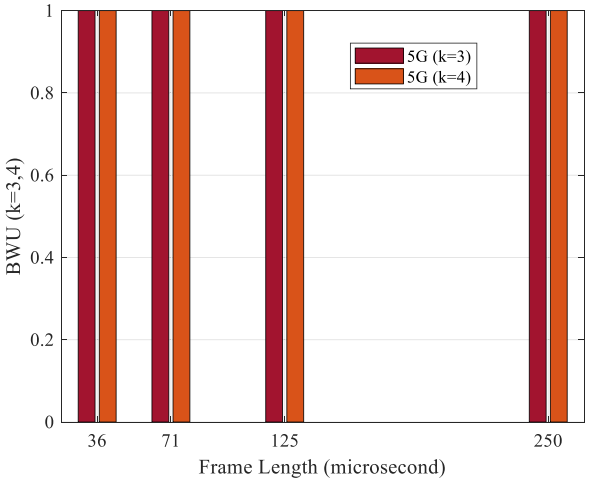

FIGURE 20. BWU of the 3rd and 4th lanes (k=3, 4).

optical access to cut-edge radio access. A multi-OLT PON-based access network is designed, in this paper, to support 5G C-RAN fronthaul along with ongoing access services. A novel DWBA scheme named ACP-2D is proposed to handle the designed access network challenges. The main objective of the scheme is to transmit 5G service reliably satisfying delay requirements along with other service types. In the proposed ONU structure, 5G service can leverage dynamic channel bonding to achieve a peak rate if necessary. The performance of the proposed DWBA is evaluated through computer simulations. Therefore, the proposed multi-OLT multi-lane PON-based OAN can adeptly satisfy the multi-access performance. The 5G delay requirement of 250 μsec (recommended by 3GPP) is achieved by satisfying the desired throughput demand in a 100 Gb/s PON system using the proposed DWBA scheme. The network delivers other services as well satisfactorily. Additionally, the network upstream bandwidth utilization is achieved around 99.9%. This work is supposed to put innovative milestones in PON-based mobile fronthaul studies.

REFERENCES

[1] F. Rawshan, M. Hossen, M. R. Islam, and Y. Park, "Multi-OLT PON-based open access network for multi-service performance tuning via the event-horizon algorithm," *J. Opt. Commun. Netw.*, vol. 15, no. 4, pp. 229–240, Apr. 2023.

[2] M. Z. Chowdhury, M. Shahjalal, S. Ahmed, and Y. M. Jang, "6G wireless communication systems: Applications, requirements, technologies, challenges, and research directions," *IEEE Open J. Commun. Soc.*, vol. 1, pp. 957–975, 2020.

[3] J. I. Kani, J. Terada, K. I. Suzuki, and A. Otaka, "Solutions for future mobile fronthaul and access-network convergence," *J. Lightw. Technol.*, vol. 35, no. 3, pp. 527–534, Feb. 1, 2017.

[4] S. S. Jaffer, A. Hussain, M. A. Qureshi, and W. S. Khawaja, "Towards the shifting of 5G front haul traffic on passive optical network," *Wireless Pers. Commun.*, vol. 112, pp. 1549–1568, Jun. 2020.

[5] X. Liu and F. Effenberger, "Emerging optical access network technologies for 5G wireless [invited]," *J. Opt. Commun. Netw.*, vol. 8, no. 12, pp. B70–B79, Dec. 2016.

[6] A. Pizzinat, P. Chanclou, F. Saliou, and T. Diallo, "Things you should know about fronthaul," *J. Lightw. Technol.*, vol. 33, no. 5, pp. 1077–1083, Mar. 1, 2015.

[7] P. Chanclou et al., "How does passive optical network tackle radio access network evolution?" *IEEE/OSA J. Opt. Commun. Netw.*, vol. 9, no. 11, pp. 1030–1040, Nov. 2017.

[8] B. Powell and E. Harstead, "25G/50G/100G EPON architectures: 1+3 vs. 1+4," Task Force Meet., San Diego, CA, USA, document IEEE P802.3ca, Jul. 2016.

[9] G. Kramer, *Ethernet Passive Optical Networks*. New York, NY, USA: McGraw-Hill, 2005.

[10] J. S. Wey, Y. Luo, and T. Pfeiffer, "5G wireless transport in a PON context: An overview," *IEEE Commun. Stand. Mag.*, vol. 4, no. 1, pp. 50–56, Mar. 2020.

[11] F. Rawshan and Y. Park, "Architecture of multi-OLT PON systems and its bandwidth allocation algorithms," *Photon. Netw. Commun.*, vol. 25, pp. 95–104, Feb. 2013.

[12] M. K. Motalleb, V. S. Mansouri, S. Parsaeefard, and O. L. A. López, "Resource allocation in an open RAN system using network slicing," *IEEE Trans. Netw. Service Manag.*, vol. 20, no. 1, pp. 471–485, Mar. 2023.

[13] M. Hossen and M. Hanawa, "Dynamic bandwidth allocation algorithm with proper guard time management over multi-OLT PON-based hybrid FTTH and wireless sensor networks," *J. Opt. Commun. Netw.*, vol. 5, no. 7, pp. 802–812, Jul. 2013.

[14] M. Hossen and M. Hanawa, "Multi-OLT and multi-wavelength PON-based open access network for improving the throughput and quality of services," *Opt. Switch. Netw.*, vol. 15, pp. 148–159, Jan. 2015.

[15] F. Rawshan and Y. Park, "Fault-tolerable and SLA-supportive architecture for TWDM-PON systems," *Photon. Netw. Commun.*, vol. 30, pp. 143–149, Apr. 2015.

[16] *IEEE Standard for Ethernet Amendment 9: Physical Layer Specifications and Management Parameters for 25 Gb/s and 50 Gb/s Passive Optical Networks*, Standard IEEE Std 802.3ca-2020 (Amendment to IEEE Std 802.3-2018 as amended by IEEE 802.3cb-2018, IEEE 802.3bt-2018, IEEE 802.3cd-2018, IEEE 802.3cn-2019, IEEE 802.3cg-2019, IEEE 802.3cq-2020, IEEE 802.3cm-2020, and IEEE 802.3ch-2020), Jul. 2020.

[17] F. Effenberger and D. Remein, "Bonding requirements for 100G-EPON," Task Force Meet., Macau, China, document IEEE P802.3ca, Mar. 2016.

[18] T. Tashiro et al., "A novel DBA scheme for TDM-PON based mobile fronthaul," in *Proc. Opt. Fiber Commun. (OFC) Conf.*, San Francisco, CA, USA, 2014, pp. 1–3.

[19] H. Uzawa et al., "Practical mobile-DBA scheme considering data arrival period for 5G mobile fronthaul with TDM-PON," in *Proc. Eur. Conf. Opt. Commun.*, Gothenburg, Sweden, 2017, pp. 1–3.

[20] D. Hisano et al., "TDM-PON for accommodating TDD-based fronthaul and secondary services," *J. Lightw. Technol.*, vol. 35, no. 14, pp. 2788–2796, Jul. 15, 2017.

[21] D. Hisano, H. Uzawa, Y. Nakayama, T. Shimada, J. Terada, and A. Otaka, "TDD pattern estimation and auto-recovery from estimation error for accommodations of fronthaul and secondary services in TDM-PON," *J. Opt. Commun. Netw.*, vol. 10, no. 2, pp. 104–113, Feb. 2018.

[22] Y. Nakayama and D. Hisano, "Wavelength and bandwidth allocation for mobile fronthaul in TWDM-PON," *IEEE Trans. Commun.*, vol. 67, no. 11, pp. 7642–7655, Nov. 2019.

[23] H. Uzawa et al., "Dynamic bandwidth allocation scheme for network-slicing-based TDM-PON toward the beyond-5G era," *J. Opt. Commun. Netw.*, vol. 12, no. 2, pp. A135–A143, Feb. 2020.

[24] A. Zaouga, A. F. de Sousa, M. Najjar, and P. P. Monteiro, "Self-adjusting DBA algorithm for next generation PONs (NG-PONs) to support 5G fronthaul and data services," *J. Lightw. Technol.*, vol. 39, no. 7, pp. 1913–1924, Apr. 1, 2021.

[25] A. Zaouga, A. De Sousa, M. Najjar, and P. P. Monteiro, "Dynamic bandwidth allocation for NG-PONs with channel bonding," *IEEE Commun. Lett.*, vol. 26, no. 2, pp. 374–378, Feb. 2022.

[26] J. Zhang, X. Liu, M. Liang, H. Yu, and Y. Ji, "Low latency DWBA scheme for mini-slot based 5G new radio in a fixed and mobile converged TWDM-PON," *J. Lightw. Technol.*, vol. 40, no. 1, pp. 3–13, Jan. 1, 2022.

[27] L. Wang et al., "Dynamic bandwidth and wavelength allocation scheme for next-generation wavelength-agile EPON," *J. Opt. Commun. Netw.*, vol. 9, no. 3, pp. B33–B42, Mar. 2017.

[28] S. B. Hussain, W. Hu, H. Xin, and A. M. Mikaeil, "Low-latency dynamic wavelength and bandwidth allocation algorithm for NG-EPON," *J. Opt. Commun. Netw.*, vol. 9, no. 12, pp. 1108–1115, Dec. 2017.
[29] S. B. Hussain, W. Hu, H. Xin, A. M. Mikaeil, and A. Sultan, "Flexible wavelength and dynamic bandwidth allocation for NG-EPONs," *J. Opt. Commun. Netw.*, vol. 10, no. 6, pp. 643–652, Jun. 2018.
[30] W. Wang, W. Guo, and W. Hu, "Dynamic wavelength and bandwidth allocation algorithms for mitigating frame reordering in NG-EPON," *J. Opt. Commun. Netw.*, vol. 10, no. 3, pp. 220–228, Mar. 2018.
[31] A. Fayad, T. Cinkler, and J. Rak, "5G/6G optical fronthaul modeling: Cost and energy consumption assessment," *J. Opt. Commun. Netw.*, vol. 15, no. 9, pp. D33–D46, Sep. 2023.
[32] J. Maes, S. Bidkar, M. Straub, T. Pfeiffer, and R. Bonk, "Efficient transport of enhanced CPRI fronthaul over PON [Invited]," *J. Opt. Commun. Netw.*, vol. 16, no. 2, pp. A136–A142, Feb. 2024.
[33] A. Rafiq, M. F. Hayat, and M. U. Younus, "Dynamic bandwidth allocation algorithm for avoiding frame rearrangement in NG-EPON," *Opt. Switch. Netw.*, vol. 43, Feb. 2022, Art. no. 100645.
[34] J. Hui, C. Gan, L. Wu, and Z. Xu, "High bandwidth utilization DWBA algorithm for upstream channel in NG-EPON," *IEEE Access*, vol. 10, pp. 99435–99444, 2022.
[35] K. N. B. Wali and M. Hossen, "Dynamic wavelength and bandwidth allocation algorithm in NG-EPON by serving ONUs request in sequential order," in *Proc. Int. Conf. Electr. Inf. Commun. Technol. (EICT)*, 2023, pp. 1–4.
[36] Y. Luo et al., "Time-and wavelength-division multiplexed passive optical network (TWDM-PON) for next-generation PON stage 2 (NG-PON2)," *J. Lightw. Technol.*, vol. 31, no. 4, pp. 587–593, Feb. 15, 2013.
[37] Y. Guo, "NG-EPON: Considerations on architecture," Task Force Meet., Atlanta, GA, USA, document IEEE P802.3ca, Jan. 2016.
[38] Y. Dai, "Manage colors for 100Gb/s EPON," Task Force Meet., Atlanta, GA, USA, document IEEE P802.3ca, Jan. 2016.

FAHMIDA RAWSHAN (Member, IEEE) received the B.Sc. degree in electrical and electronic engineering (EEE) from the Rajshahi University of Engineering and Technology, Bangladesh, in 2009, and the M.Sc. degree in electronics engineering from Kookmin University, South Korea, in 2012. She is currently pursuing the Ph.D. degree with the Department of EEE, Khulna University of Engineering and Technology, Bangladesh, and receiving the prestigious University Grand Commission Ph.D. Fellowship. She was involved in many Korean government projects from 2010 to 2012. Her research interests include PON, IoT, WSN, and optical communication. In 2012, she received the Excellent Student Award from Kookmin University.

MONIR HOSSEN (Senior Member, IEEE) received the B.Sc. degree in EEE from the Khulna University of Engineering and Technology (KUET), Bangladesh, in 2002, the M.Sc. degree in EE from Kookmin University, South Korea, in 2010, and the Ph.D. degree from the University of Yamanashi, Japan, in 2014. He is currently working as a Professor with the Department of Electronics and Communication Engineering, KUET. His current research focuses on MAC protocol of WSN, vehicular ad-hoc network, and PON.

MD. RAFIQUL ISLAM (Member, IEEE) received the B.Sc. degree in EEE from the Khulna University of Engineering and Technology (KUET), Bangladesh, in 1991, the M.Sc. degree in EEE from the Bangladesh University of Engineering and Technology, Bangladesh, in 1998, and the D.Eng. degree from the Kyoto Institute of Technology, Japan, in 2004. He is currently working as a Professor with the Department of EEE, KUET. He has published about 150 research papers in different journals and international conferences. He is an owner of a patent titled "Energy Meter With Automatic Load Management." His current research interests include optoelectronic devices, optical communications and networks, and smartphone-based instrumentation.